Published in final edited form as:
*Int J Radiat Oncol Biol Phys*. 2008 January 1; 70(1): 154–160. doi:10.1016/j.ijrobp.2007.05.078.

# LIVER FUNCTION AFTER IRRADIATION BASED UPON CT PORTAL VEIN PERFUSION IMAGING

**Yue Cao, Ph.D.**[1,2], **Charlie Pan, MD**[1], **James M. Balter, Ph.D.**[1], **Joel F. Platt, MD**[2], **Isaac R. Francis, MD**[2], **James A. Knol, MD**[3], **Daniel Normolle, Ph.D.**[1], **Edgar Ben-Josef, MD**[1], **Randall K. Ten Haken, Ph.D.**[1], and **Theodore S. Lawrence, MD, Ph.D.**[1]

[1] Department of Radiation Oncology, University of Michigan, Ann Arbor, MI, USA

[2] Department of Radiology, University of Michigan, Ann Arbor, MI, USA

[3] Department of Surgery, University of Michigan, Ann Arbor, MI, USA

## Abstract

**Purpose—**The role of radiation in the treatment of intrahepatic cancer is limited by the development of radiation-induced liver disease (RILD), which occurs weeks after the course of radiation is completed. We hypothesized that, as the pathophysiology of RILD is veno-occlusive disease, we could assess *individual and regional liver* sensitivity to radiation by measuring liver perfusion during a course of treatment using dynamic contrast enhanced CT (DCE-CT) scanning.

**Materials and Methods—**Patients with intrahepatic cancer undergoing conformal radiotherapy underwent DCE-CT (to measure perfusion distribution) and an indocyanine extraction study (to measure liver function) prior to, during, and one month after treatment. We wished to determine if the residual functioning liver (i.e. those regions showing portal vein perfusion) could be used to predict overall liver function after irradiation.

**Results—**Radiation doses from 45 to 84 Gy resulted in undectable regional portal vein perfusion one month after treatment. The volume of each liver with undectable portal vein perfusion ranged from 0% to 39% and depended both on the patient's sensitivity and dose distribution. There was a significant correlation between indocyanine green clearance and the mean of the estimated portal vein perfusion in the functional liver parenchyma ($P < .001$).

**Conclusion—**This study reveals substantial individual variability in the sensitivity of the liver to irradiation. In addition, these findings suggest that hepatic perfusion imaging may be a marker for liver function, and has the potential to be a tool for individualizing therapy.

### Keywords

liver function; hepatic perfusion; radiation-induced liver disease; intrahepatic cancer; individual radiation sensitivity

Corresponding Author: Yue Cao, Ph.D., University of Michigan, Departments of Radiation Oncology and Radiology, UH-B2C432, Box 0010, Ann Arbor, MI 48109-0010, Phone: (734)647-2914, Fax: (734)936-7859, Email: E-mail: yuecao@umich.edu.

This work has not been presented anywhere. However, an abstract has been submitted for presentation in the 2007 annual meeting of ASTRO.

Conflicts of Interest Notification:
None of authors has any actual or potential conflicts of interest related to this study.

## INTRODUCTION

High-dose conformal radiation therapy (RT) used in combination with chemotherapy appears to prolong the survival of patients with unresectable intrahepatic cancers.[1] Unfortunately, attempts to increase the radiation dose have been limited by the development of radiation-induced liver disease (RILD), often called radiation hepatitis, in some patients.[2] The symptoms of RILD typically begin to occur one to two months after the completion of RT. The pathologic changes of RILD include veno-occlusive disease (VOD), which is characterized by thrombosis within the central veins of the liver producing post hepatic congestion.[3] A tool that could be used for the early detection of RILD would help facilitate individualized therapy by permitting the early cessation of treatment in patients who were developing toxicity and permitting higher doses of radiation for patients with no signs of ill effects. If, in addition, there were information about the specific regions of the liver that were being injured, it would be possible to consider redesigning radiation fields during a course of treatment to avoid further injury. Such individualization would likely improve outcomes as welll as patient quality of life.

Although there are currently no routine methods of estimating local function within the liver, there are established methods of measuring whole liver function. Probably the best-studied method of measuring liver function is through assessing the extraction of Indocyanine green (ICG).[4–7] After intravenous administration, ICG dye is taken up from the plasma almost exclusively by the hepatic parenchymal cells and is secreted into the bile. It undergoes no significant extrahepatic or enterohepatic circulation. Simultaneous arterial and venous blood estimations have shown negligible renal, peripheral, lung, or cerebro-spinal uptake of the dye. Therefore, the serum clearance rate of ICG serves as a reliable index of liver function. The clinical value of the ICG test has been demonstrated in the evaluation of donor organs for transplantation and the outcome of liver resections.[4–7] Also, the ICG test was reported to be an early indicator of hepatic dysfunction following injury, in which the prolonged ICG clearance preceded an increase in serum bilirubin levels.[4]

Based upon the biological mechanism of RILD, we previously proposed a regional perfusion and local dose model for the prediction of local venous perfusion dysfunction.[8] In this model, the reduction of regional portal vein perfusion for individual patients after RT was predicted by the dose to that region and the perfusion measured prior to the end of RT. This finding suggested that individual sensitivity to radiation coupled with the distribution of dose delivery to the liver parenchyma determine regional dysfunction.

Based on these studies, we hypothesized that measurements of liver perfusion during treatment could, when combined with the 3D dose distribution in normal liver, predict not simply liver blood flow after treatment, but actual liver function. To test this hypothesis, we conducted a pilot study to compare the effect of radiation on liver perfusion (using DCE-CT) to overall liver function (measured by IC-Green) after treatment.

## METHODS

### Patients

Eleven patients (3 women and 8 men, age from 35 to 79 years) with unresectable intrahepatic cancer (1 with hepatocellular carcinoma, 5 with cholangiocarcinoma, and 5 with colorectal carcinoma metastatic to the liver) participated in an IRB-approved liver contrast enhanced CT perfusion study. Ten patients were also enrolled in a separate IRB-approved ICG study. All patients signed written consents prior to enrollment. Patients were treated using three-dimensional conformal RT techniques. The median dose of radiation delivered to tumor was 67.5 Gy (range 48–78 Gy). Ten patients received concurrent continuous infusion hepatic artery

floxuridine, and one patient was treated with concurrent capecitabine. Only one patient (#1) developed RILD after RT.

**ICG Clearance Test—**The ICG clearance test was administrated prior to RT, after delivery of ~22 Gy and ~45 Gy to tumor, and one month after the completion of RT. The test was performed in a standard fashion. Briefly, patients were asked not to eat the morning of the test, but were allowed coffee and/or water up to approximately two hours before the test. Patients were to take all of their medications as usual. Each patient had two different intravenous (IV) catheters: one for the ICG infusion, and the other for drawing samples. Following a rapid IV push ICG dye (0.5 mg/kg), a 6-cc blood sample was drawn at time 0. Additional serum samples were collected at approximately 5, 10, 15, and 20 minutes after IV injection of the dye. Each blood sample was approximately 6 cc. Catheters were flushed with saline following each blood draw. The half-life time (T1/2) of ICG clearance was estimated from the serum samples.

## Liver Perfusion

Computed tomography liver perfusion scans were performed prior to RT, after delivery of ~22 Gy and ~45 Gy to tumor, and one month after the completion of RT. The CT perfusion protocol, methodologies for estimation of hepatic perfusion, and characteristic changes in portal vein perfusion during and after RT have been previously described.[8, 9] The relevant information for this analysis will be described briefly. Hepatic artery perfusion and portal vein perfusion (Fp) were estimated in an axial plane extending over a 2-cm thick slab in the cranial-caudal direction and covering the entrance of the main portal vein into the liver, the hepatic artery, a portion of liver parenchyma, and, if possible, a portion of the tumor.[8] After registration of each perfusion CT with its corresponding treatment planning CT, dose distributions (or iso-dose regions) were overlaid on portal vein perfusion images for further analysis.

## Portal Vein Perfusion Dose-Response Function

The relationship between the regional portal vein perfusion one month after RT and the local dose accumulated up to the end of RT (venous perfusion dose-response function – VPDRF) was evaluated from multiple volumes of interest within the liver. Care was taken to exclude artifacts, large vessels, and gross tumor volume from these volumes of interest. The sizes of the volumes of interest ranged from 0.5 to 7.5 cc with a median of 2.5 cc, depending upon the spatial dose distributions in the 2-cm slab. The mean doses and the mean venous perfusion values were calculated in each of the volumes of interest for determination of the VPDRF.

The individual VPDRF in the 2-cm slab for each patient was analyzed by linear regression to yield a slope and intercept (Figure 1, Appendix). From individual VPDRFs, we determined critical doses resulting in zero portal vein perfusion (see Appendix), which represented the individual sensitivity to radiation. In order to provide an estimate of portal vein perfusion in the entire normal liver for each patient, the VPDRF was applied to the treatment planning dose at each liver voxel location outside the 2 cm slab.

## Liver Residual Function Estimated by Liver Perfusion

We also tested whether the residual liver function estimated by venous perfusion could be used as a marker for the overall liver function after RT. We formulated a metric, the mean of the portal vein perfusion over the whole liver parenchyma, as a measure of the residual liver function (Appendix). We then performed a linear regression of the half-life time (T1/2) of ICG clearance and this metric. The strength of this correlation was compared to that of mean hepatic radiation dose versus ICG clearance time.

### Analysis of Critical Perfusion Values for Regional Functioning Liver

Anticipating that the damaged liver regions, indicated by undectable or low portal vein perfusion, would not contribute to liver function, we performed sensitivity analyses to assess the critical value of portal vein perfusion below which the subunits of the liver parenchyma would not contribute to liver function. We sequentially excluded voxels with portal vein perfusion values less than 0, 10, 20, 30, 40, and 50 mL/(100 g min) from the computation of the residual liver function. We then tested the correlation between each of the residual liver functions and the T1/2 of ICG clearance by linear regression. The critical portal vein perfusion, below which the subunits of the liver parenchyma do not contribute to liver residual function, was obtained from the threshold which yielded the best correlation between the tested residual liver function and the T1/2 of ICG clearance. Finally, the corresponding critical dose was obtained from the critical portal vein perfusion and the individual VPDRF for each patient.

## RESULTS

### Portal Vein Perfusion Dose-Response Function

We began to establish a model for the prediction of spatially-distributed hepatic perfusion over the whole liver after RT by using the perfusion data acquired in a 2-cm slab. Figure 1 shows examples of the individual VPDRFs. The linear fittings of the individual patients' regional portal vein perfusion and local dose measured in the single slab one month after RT resulted in a slope (*A*) and the intercept (*B*) for each patient (Table 1). All fits were statistically significant (*P* values: < .05 to .001), except for the one patient who developed RILD after RT. The intercept, *B*, is interpreted as portal vein perfusion at zero dose. The values of B were greater than the means of the portal vein perfusion observed prior to RT in eight (73%) patients (Table 1). This suggests that portal vein perfusion in the low dose region may compensate for the loss of portal vein perfusion in the high dose region. The critical doses for zero portal vein perfusion estimated by the VPDRF ranged from 45.5 to 84.4 Gy with a median of 59.9 Gy, indicating a large variation in individual sensitivity to radiation dose (Table 2).

Extension of the VPDRF from the 2-cm slab to the volume of the whole liver parenchyma via the total dose distribution resulted in estimates of the spatially-distributed portal vein perfusion over the whole liver (Figure 2). From those total liver distributions, the fractional volumes of the liver parenchyma having zero portal vein perfusion were computed with resulting values ranging from 0% to 39%, depending on the individual sensitivity to dose and the liver dose distribution of the treatment plan (Table 2).

For the patient who developed RILD after RT, portal vein perfusion one month after RT was reduced to less than 10 mL/(100 g min) in the axial slab (mean = 4.5 mL/100g min), which was substantially lower than in other patients. Also, the residual portal venous perfusion observed in the slab lost dose-dependency.

### Correlation of the Residual Liver Function with the ICG Clearance after RT

The calculated means of portal vein perfusion over the whole liver parenchyma one month after RT for each patient are reported in Table 3, as are each patient's T1/2 of ICG clearance one month after RT. We found that the means of portal vein perfusion were linearly correlated with the T1/2s of ICG clearance ($r = 0.85$, $P < .005$, left panel of Figure 3), suggesting that the spatially-resolved portal vein perfusion may be a marker for overall liver function one to two months after RT. In contrast, the correlation between the mean dose in the liver parenchyma and the T1/2 of the ICG clearance was not significant ($r = 0.31$, $P > .4$, Figure 4), indicating that mean liver dose alone does not do well in predicting liver function (as indicated by ICG clearance) after RT.

### Critical Portal Vein Perfusion for Liver Function

By sequentially eliminating the voxels having $F_p \leq 0$, 10, 20, 30, 40, and 50 mL/(100 g min) from the computation of residual liver function, we found that the best correlation between ICG clearance and the means of portal vein perfusion was found when excluding voxels with $F_p \leq 20$ mL/(100 g min) from the calculation of the mean ($r = 0.94$, $P < .001$, Figure 3). This supports the assumption that a damaged liver subunit having low portal vein perfusion would not contribute to overall liver function. The dose that decreases portal vein perfusion to 20 mL/(100 g min) ranged from 42.4 to 67.8 Gy in the patients with a median dose of 54.4 Gy (Table 2), indicating there is a greater risk for the patients who have higher sensitivity to radiation and in which a larger portion of the liver received the dose above the critical value.

## DISCUSSION

This study examined patients with unresectable intrahepatic cancers who underwent 3D conformational RT and assessed the individual sensitivity of liver parenchyma to radiation by analyzing the relationship between regional portal vein perfusion one month after RT and the local dose accumulated to the end of RT. The analyses reveal that there are individualized venous perfusion dose response functions, VPDRFs. Subsequently, there are also individualized critical doses that result in regional venous perfusion dysfunction indicated by zero or low portal vein perfusion, for which the liver subunits are assumed to not contribute to overall liver function. Further, we tested the mean of portal vein perfusion over the whole liver parenchyma as a measure of the overall liver residual function by performing correlative analysis with the half-life time of ICG clearance, and found it to be highly predictive. We demonstrate that the residual liver function depends on the distribution of the dose delivered to the liver, along with the venous perfusion dose-response function. The latter function represents an individual's risk to radiation.

Individual patient sensitivity to RILD after RT has been recognized clinically; however, accurately predicting individual sensitivity to radiation before or during treatment remains a challenge. Several clinical and patient-specific factors have been identified that may influence the incidence of RILD in patients who undergo intrahepatic RT.[10–13] Analyses of the incidences of RILD using a NTCP model reveal that the susceptibility to RILD is different for patients who have metastases, and primary liver tumors with and without Child Pugh B cirrhosis.[10, 13] Subsequently, these clinical factors have been used for modification of NTCP models to improve dose prescription and to reduce the risk of development of RILD in patients with these clinical conditions.[10, 13] However, individual deviation from the prediction of the population or sub-population based models can result in an increase in risk for development of RILD or missing the opportunity for safe delivery of higher dose to the tumor. Assessing and predicting individual sensitivity to radiation by a biomarker such as imaging prior to the end of treatment could greatly aid the successful application of individualized therapy.

Here, via analysis of individual VPDRFs, we identified a range of individual sensitivities to dose (Tables 2 and 3). These individual sensitivities to radiation, together with the dose distribution of the liver, appear to correlate with the residual liver function after RT. We established a significant correlation between the overall liver function assessed by the ICG clearance test and the residual liver function based upon spatially-distributed portal vein perfusion after RT. We used the concept that the liver can be modeled reasonably well as a parallel organ.[10, 14–16] In this regard, the overall function of the liver is considered to be carried out by the portion of liver that remains undamaged, and a patient will not develop RILD as long as this undamaged portion of the liver maintains a sufficient volume. Thus, we formulated the residual liver function after RT as a mean of spatially-distributed portal vein perfusion over the whole liver parenchyma. Our analysis shows that the volume-weighted mean of portal vein perfusion in the portion of the liver parenchyma retaining a minimum level (~20 mL/100 g

min) of venous perfusion correlates with the ICG clearance test results. This correlation suggests that radiation damage to the liver within one to two months after the completion of RT may be predominantly vascular injury. Therefore, spatially-distributed portal vein perfusion may be a marker for the spatially-distributed liver function and the overall liver function within this time frame. We note that previous studies of radiation-induced "lung" injury have reported the correlation between the pulmonary function test and the sum of the reduction in regional SPECT perfusion in the lung after RT.[17–22] We extended the general concept presented by these studies to evaluate a test protocol to predict individual patient residual liver function after RT.

The findings suggest a new tool for radiation treatment planning and re-optimization of the plan during therapy for intrahepatic radiation treatment. Conventionally, the mean liver dose is determined based upon the prediction of the likelihood of RILD by the NTCP model, and is used for the optimization of treatment planning. In light of our analysis, the estimated impact of the dose distribution of the liver from the initial treatment plan could be evaluated by estimating portal vein perfusion distribution after irradiation based upon the averaged portal vein perfusion dose-response function of the population. Then, the residual liver function that can be estimated from the portal vein perfusion distribution could be assessed as to whether it is greater than a critical value, which defines the tolerable level of RILD incidences. Re-evaluation of the radiation treatment plan could be further carried out during therapy, possibly two-thirds of the way into the treatment, based upon the assessment of the patient's individual portal vein perfusion dose-response function. If the predicted residual liver function after RT is too low, indicating high risk for RILD, the treatment plan could be adjusted.

This study has several limitations. First, the spatially-distributed portal vein perfusion over the whole liver parenchyma is estimated from the measurements obtained from a 2-cm slab. Thus, the findings relating the spatial-distributed portal vein perfusion to the overall liver function need to be verified in volumetric measurements of portal vein perfusion. Second, the correlation between the ICG clearance values and the liver residual function based on the venous perfusion needs to be re-confirmed in a larger number of patients with and without RILD. Third, we observed an increase in portal vein perfusion in the regions that received low dose, suggesting that these regions may compensate for the loss and the reduction of portal vein perfusion in the regions that received high dose. Thus, the low-dose regions cannot be used for normalization or control. The extent of the increase needs to be evaluated in a large number of patients using volumetric perfusion imaging. Fourth, we used the physical dose in the individual VPDRF for the computation of the residual liver function. In our previous study, we reported that the linear-quadratic model correction for local fraction size did not make any significant difference in the fittings of the VPDRFs. However, the linear-quadratic equation, which is based upon the observation of cell survival, may or may not apply to radiation-induced vascular injury in the liver and moreover, the VPDRF is fitted well by linear regression. Studies are ongoing in a larger patient group using 3D MRI perfusion imaging to resolve many of these outstanding issues.

In conclusion, we previously demonstrated that regional venous perfusion dysfunction after RT was predicted by local accumulated dose and the perfusion measured prior to the end of RT, suggesting a new strategy for studying radiation toxicity in the liver and providing an opportunity for individualized therapy to patients with intrahepatic cancer.[8] To further develop this new paradigm, we assessed individual sensitivity to radiation by analyzing the individual portal vein perfusion dose-response function and the critical dose that resulted in portal venous perfusion dysfunction. Furthermore, we demonstrated a significant correlation between the best-established liver function index—ICG clearance, and the residual liver function based upon the spatially-distributed portal vein perfusion over the liver parenchyma after RT. Our analyses suggest that hepatic perfusion imaging may be a marker for liver function, yielding

a new risk assessment strategy that has great potential as an effective tool for individualized therapy.

## Acknowledgments

This work was supported in part by 3 PO1 CA59827.

## References

1. Ben-Josef E, Normolle D, Ensminger WD, et al. Phase II trial of high-dose conformal radiation therapy with concurrent hepatic artery floxuridine for unresectable intrahepatic malignancies. J Clin Oncol 2005;23:8739–8747. [PubMed: 16314634]
2. Emami B, Lyman J, Brown A, et al. Tolerance of normal tissue to therapeutic irradiation. Int J Radiat Oncol Biol Phys 1991;21:109–122. [PubMed: 2032882]
3. Lawrence TS, Robertson JM, Anscher MS, et al. Hepatic toxicity resulting from cancer treatment. Int J Radiat Oncol Biol Phys 1995;31:1237–1248. [PubMed: 7713785]
4. Gottlieb ME, Stratton HH, Newell JC, et al. Indocyanine green. Its use as an early indicator of hepatic dysfunction following injury in man. Arch Surg 1984;119:264–268. [PubMed: 6696619]
5. Hemming AW, Scudamore CH, Shackleton CR, et al. Indocyanine green clearance as a predictor of successful hepatic resection in cirrhotic patients. Am J Surg 1992;163:515–518. [PubMed: 1575310]
6. Oellerich M, Burdelski M, Lautz HU, et al. Assessment of pretransplant prognosis in patients with cirrhosis. Transplantation 1991;51:801–806. [PubMed: 2014533]
7. Pollack DS, Sufian S, Matsumoto T. Indocyanine green clearance in critically ill patients. Surg Gynecol Obstet 1979;149:852–854. [PubMed: 388703]
8. Cao Y, Platt JF, Francis IR, et al. The prediction of radiation-induced liver dysfunction using a local dose and regional venous perfusion model. Medical Physics 2007;33:604–612. [PubMed: 17388178]
9. Cao Y, Shen Z, Alspaugh J, et al. A practical approach for quantitative estimates of voxel-by-voxel liver perfusion using DCE imaging and a compartmental model. Medical Physics 2006;33:3057–3062. [PubMed: 16964883]
10. Dawson LA, Normolle D, Balter JM, et al. Analysis of radiation-induced liver disease using the Lyman NTCP model. Int J Radiat Oncol Biol Phys 2002;53:810–821. [PubMed: 12095546]
11. Cheng JC, Liu HS, Wu JK, et al. Inclusion of biological factors in parallel-architecture normal-tissue complication probability model for radiation-induced liver disease. Int J Radiat Oncol Biol Phys 2005;62:1150–1156. [PubMed: 15990021]
12. Cheng JC, Wu JK, Lee PC, et al. Biologic susceptibility of hepatocellular carcinoma patients treated with radiotherapy to radiation-induced liver disease. Int J Radiat Oncol Biol Phys 2004;60:1502–1509. [PubMed: 15590181]
13. Xu ZY, Liang SX, Zhu J, et al. Prediction of radiation-induced liver disease by Lyman normal-tissue complication probability model in three-dimensional conformal radiation therapy for primary liver carcinoma. Int J Radiat Oncol Biol Phys 2006;65:189–195. [PubMed: 16542787]
14. Austin-Seymour MM, Chen GT, Castro JR, et al. Dose volume histogram analysis of liver radiation tolerance. Int J Radiat Oncol Biol Phys 1986;12:31–35. [PubMed: 3080390]
15. Ten Haken RK, Martel MK, Kessler ML, et al. Use of Veff and iso-NTCP in the implementation of dose escalation protocols. Int J Radiat Oncol Biol Phys 1993;27:689–695. [PubMed: 8226166]
16. Jackson A, Ten Haken RK, Robertson JM, et al. Analysis of clinical complication data for radiation hepatitis using a parallel architecture model. Int J Radiat Oncol Biol Phys 1995;31:883–891. [PubMed: 7860402]
17. Boersma LJ, Damen EM, de Boer RW, et al. Dose-effect relations for local functional and structural changes of the lung after irradiation for malignant lymphoma. Radiother Oncol 1994;32:201–209. [PubMed: 7816939]
18. Boersma LJ, Damen EM, de Boer RW, et al. A new method to determine dose-effect relations for local lung-function changes using correlated SPECT and CT data. Radiother Oncol 1993;29:110–116. [PubMed: 8310136]

19. Boersma LJ, Damen EM, de Boer RW, et al. Estimation of overall pulmonary function after irradiation using dose-effect relations for local functional injury. Radiother Oncol 1995;36:15–23. [PubMed: 8525021]
20. Marks LB, Munley MT, Spencer DP, et al. Quantification of radiation-induced regional lung injury with perfusion imaging. Int J Radiat Oncol Biol Phys 1997;38:399–409. [PubMed: 9226329]
21. Fan M, Marks LB, Hollis D, et al. Can we predict radiation-induced changes in pulmonary function based on the sum of predicted regional dysfunction? J Clin Oncol 2001;19:543–550. [PubMed: 11208849]
22. Fan M, Marks LB, Lind P, et al. Relating radiation-induced regional lung injury to changes in pulmonary function tests. Int J Radiat Oncol Biol Phys 2001;51:311–317. [PubMed: 11567804]

## Appendix

## APPENDIX

In order to estimate spatially-distributed portal vein perfusion over the whole liver, a linearly equation such as:

$$F_p = A \times dose + B \quad [1]$$

can be fitted to portal vein perfusion ($F_p$) and local total dose accumulated at the time of the perfusion scan in the 2-cm slab, where $A$ is the slope and $B$ is the intercept of the linear regression. From Equation [1], the dose resulting in zero portal vein perfusion for each patient, defined as the critical dose, $-B/A$ using Equation [1], is calculated.

## Residual Liver Function Estimated by Liver Perfusion

A metric of the mean portal vein perfusion over the whole liver parenchyma is formulated as a potential measure of the residual liver function, and is calculated as:

$$\text{residual liver function} = \overline{F_p} = \frac{\sum_i F_p(i)\Delta v}{\sum_i \Delta v} = \frac{1}{N}\sum_i F_p(i), \quad [2]$$

where $F_p(i)$ is the portal vein perfusion at voxel $i$, and $N$ is the number of voxels in the volume of the whole liver parenchyma (the whole liver minus the gross tumor volume). The metric can also be interpreted as the volume-weighted venous perfusion over the whole liver parenchyma.

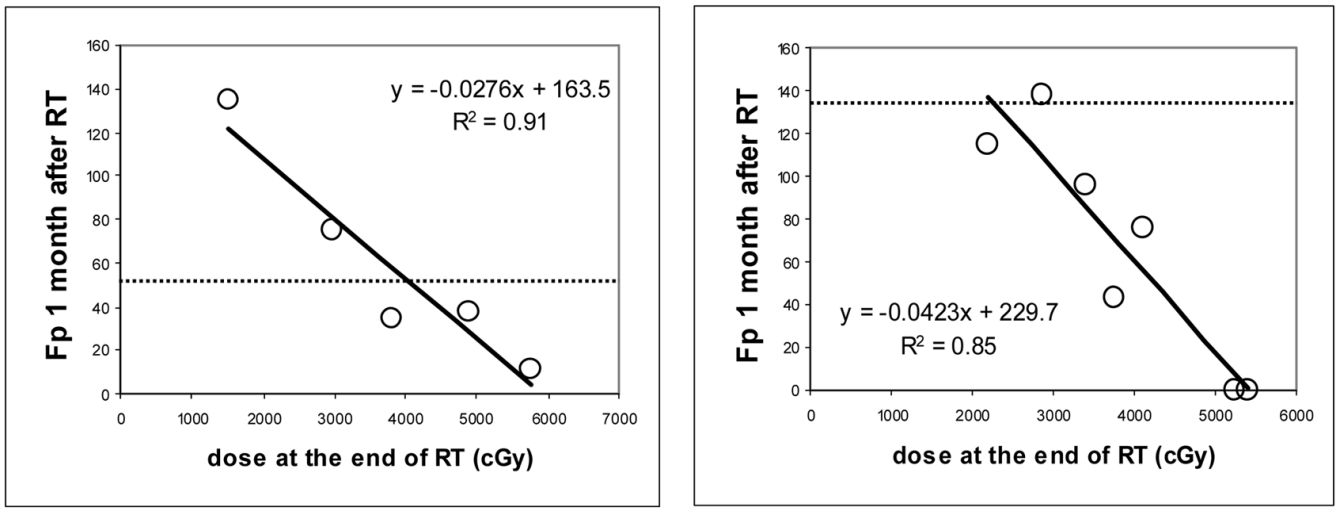


**Figure 1.**

Scatter plots of regional portal vein perfusion (mL/(100g min)) one month after the completion of RT versus local dose (cGy) accumulated at the end of RT in two patients (open circles). The solid lines plot linear regression fits. The dashed lines represent the portal vein perfusion values prior to RT. Note that the values of portal vein perfusion prior to RT are smaller than the intercepts of linear regression, suggesting that while high dose causes a decrease in perfusion, low dose can result in an increase.

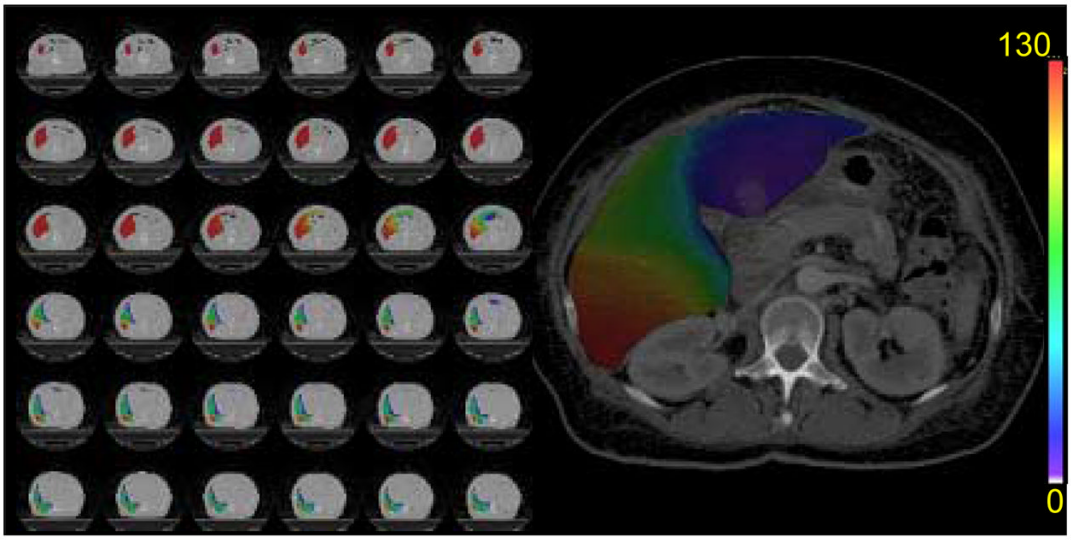


**Figure 2.**
Spatial distribution of estimated portal vein perfusion in the whole liver parenchyma one month after RT in one patient. Portal vein perfusion is color-coded (in unit of mL/(100 g min)) and overlaid on the anatomical CT.

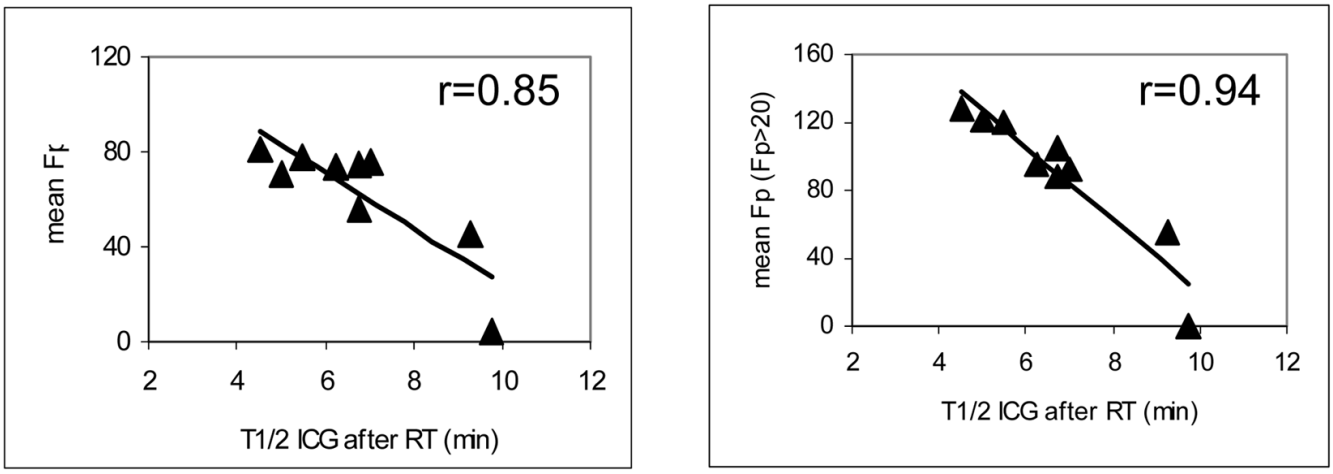


**Figure 3.**

Linear correlations between the means of the estimated portal vein perfusion versus the half-life time of the ICG clearance one month after RT. In the left panel, the mean of portal vein perfusion was computed in the whole liver parenchyma (minus the gross tumor volume), while in the right panel only subunits having venous perfusion > 20 mL/(100 g min) were included in the mean. The solid lines represent the linear regression fit. The mean perfusion is in units of mL/(100 g min).

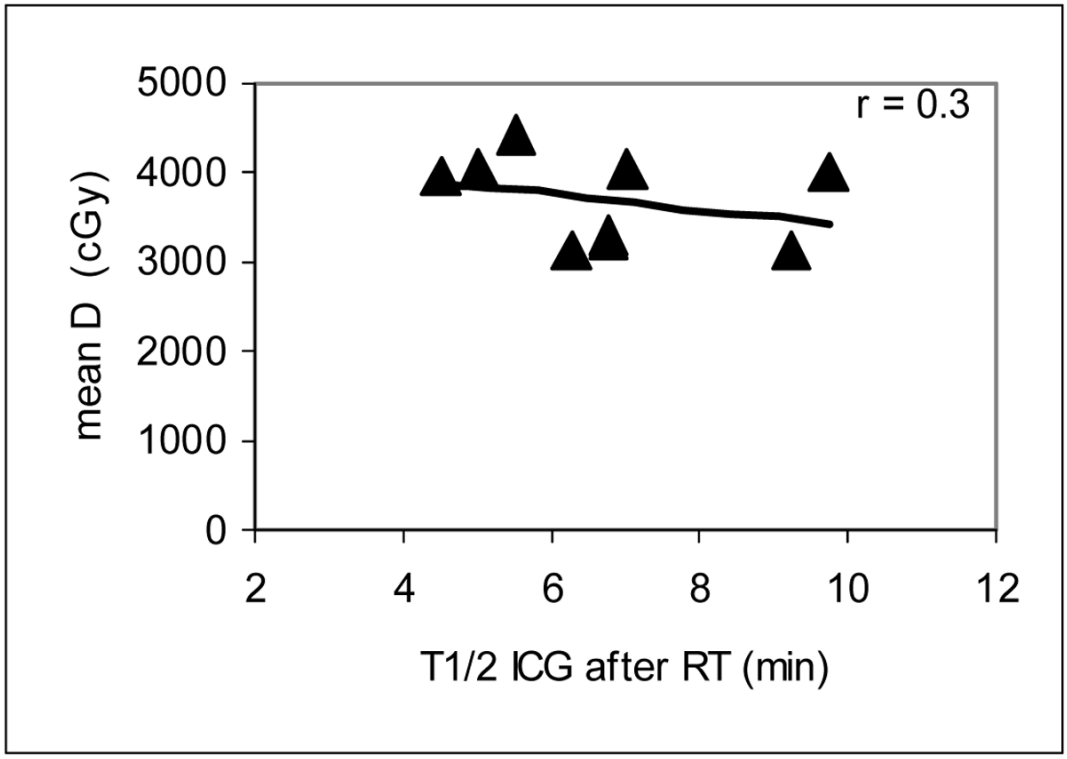


**Figure 4.**
Scatter plot of the mean liver dose (cGy) versus the half-life of the ICG clearance (minutes) one month after RT. The correlation between the mean liver dose and the half-life of the ICG clearance was not significant ($P > .4$), suggesting the mean liver dose cannot accurately predict liver function after RT.

**Table 1**

Parameters for Portal Vein Perfusion Dose-Response Function

| | **Linear Model Fp one month post RT Fp=A*dose+B** | | **Mean Fp pre RT (mL/(100 g min))** |
|---|---|---|---|
| **Patients** | **Slope A (mL/(100 g min) per Gy)** | **Intercept B (ml/100 g min)** | |
| 1 | NA | NA | 97.1 |
| 2 | −2.56 | 153.2 | 55.7 |
| 3 | −3.19 | 161.4 | 53.4 |
| 4 | −2.23 | 141.4 | 79.1 |
| 5 | −6.46 | 293.9 | 151.0 |
| 6 | −4.15 | 248.5 | 111.4 |
| 7 | −2.78 | 187.6 | 64.3 |
| 8 | −1.07 | 78.7 | 67.2 |
| 9 | −4.23 | 229.7 | 135.0 |
| 10 | −1.30 | 105.3 | 208.3 |
| 11 | −1.20 | 101.3 | 104.3 |

**Table 2**

Critical Doses and Corresponding Fractional Volumes

| Patients | N Liver V ($\times 10^3$ $cm^3$) | Dose for Fp=0 (Gy) | V% for Fp=0 | Dose for Fp=20 (Gy) | V% for Fp<20 |
|---|---|---|---|---|---|
| 1 | 1.49 | NA | NA | NA | 100% |
| 2 | 1.84 | 59.9 | 11% | 52.0 | 24% |
| 3 | 2.29 | 50.6 | 0% | 44.3 | 42% |
| 4 | 1.45 | 63.4 | 23% | 54.4 | 30% |
| 5 | 1.41 | 45.5 | 39% | 42.4 | 42% |
| 6 | 1.54 | 59.9 | 32% | 55.1 | 35% |
| 7 | 1.37 | 67.5 | 6% | 60.3 | 19% |
| 8 | 2.16 | 73.6 | 3% | 54.9 | 19% |
| 9 | 1.76 | 54.3 | 31% | 49.6 | 37% |
| 10 | 1.26 | 81.0 | 0% | 65.6 | 0% |
| 11 | 1.64 | 84.4 | 0% | 67.8 | 17% |

Fp: portal vein perfusion in mL100 g min; dose: in Gy.

**Table 3**

Residual Liver Function and ICG Clearance After RT

| Patients | $\overline{F}_p$ (mL/(100 g min)) | T1/2 Of ICG (min) |
|---|---|---|
| 1 | 4.5 | >9.75 |
| 2 | 73.6 | 6.25 |
| 3 | 55.9 | 6.75 |
| 4 | 74.4 | 6.75 |
| 5 | 71.0 | 5.0 |
| 6 | 78.2 | 5.5 |
| 7 | 76.0 | 7.0 |
| 8 | 45.5 | 9.25 |
| 9 | 81.4 | 4.5 |
| 10 | 70.2 | incomplete |
| 11 | 64.4 | NA |